BULLETIN OF THE EARTHQUAKE
RESEARCH INSTITUTE
Vol. 44 (1966), pp. 1009-1040

51. *A Long Wave in the Vicinity of an Estuary* [III].

By Takao MOMOI,

Earthquake Research Institute.

(Read April 26, 1966.—Received June 30, 1966.)

Abstract

Succeeding the previous works under the same title, the theories on long waves around an estuary are developed under the approximations of the third, fourth, and fifth orders of the Bessel functions. A principle used in this paper is a method of the buffer domain devised by the author. The newly obtained facts are as follows:—

(1) In the interior of the canal, a valley of the amplitude is found, which was passed unnoticed in the previous works, (2) a trough line in the open sea bends down towards the mouth of the canal, which results in an entrance of a tongue-shaped valley of the amplitude inside the canal, (3) in front of the canal, isolines of phase take a trapezoid form, and (4), when $kd=1.4$ (k: a wave number, d: a half width of the canal), diverted waves appear in the open sea which advance along the straight coast causing high waves there.

1. Introduction

We have already been studying a problem of a long wave in the vicinity of an estuary[1), 2)] by use of a method of the buffer domain with the aid of an electronic computer. In this paper, the theory is developed under the third, fourth and fifth approximations. The used notations and definitions are completely the same as those in the previous papers[1), 2)] (of which the first and second works are referred to as papers I and II in the following). The summary of the definitions and notations are presented in Section 2 of paper II. If necessary in the following development of the theory, readers should refer to Section 2 of paper II.

1) T. MOMOI, *Bull. Earthq. Res. Inst.*, **43** (1965), 291-316.
2) T. MOMOI, *Bull. Earthq. Res. Inst.*, **43** (1965), 459-498.

2. Formal Solutions

In paper I, formal solutions in three domains D_1, D_2 and D_3 (refer to Fig. 1) are given as follows:—

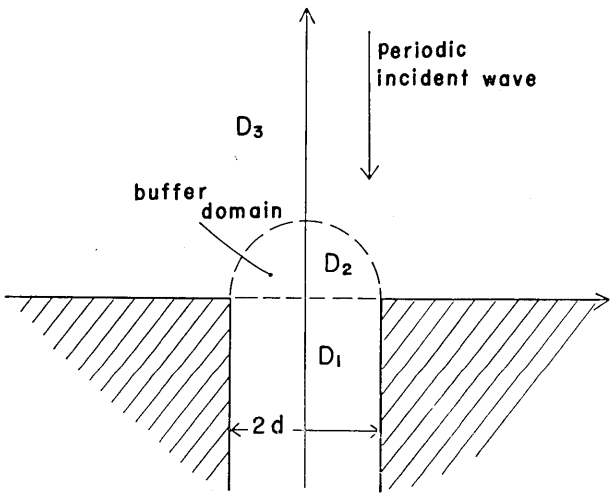

Fig. 1. A geometry of a used model.

in the domain D_1 (from (9) of paper I),

$$\zeta_1=\sum_{m=0}^{\infty}\zeta_1^{(m)}\cos\frac{m\pi}{d}x\cdot e^{-ik_1{}^{(m)}y}\,; \tag{1}$$

in the domain D_2 (from (8) of paper I),

$$\zeta_2=\sum_{n=0}^{\infty}\{\zeta_2^{(2n)}\cos 2n\theta\cdot J_{2n}(kr)+\zeta_2^{(2n+1)}\sin(2n+1)\theta\cdot J_{2n+1}(kr)\}\,; \tag{2}$$

in the domain D_3 (from (6) of paper I),

$$\zeta_3=2\zeta_0\cos ky+\sum_{n=0}^{\infty}\zeta_3^{(2n)}\cos 2n\theta\cdot H_{2n}^{(1)}(kr)\,. \tag{3}$$

3. Infinite Simultaneous Equations

Communicating the above formal expressions by use of the boundary conditions between the adjacent domains and applying the operators,

which have a property of orthogonality, to these relations (these procedures are the first reduction of the method of the buffer domain[3]), we have the following infinite simultaneous equations (For the detailed derivation of these equations, readers should refer to Section 2 of paper I):—

$$\sum_{n=0}^{\infty} I(J_{2n}, m)\cdot\overline{\zeta}_2^{(2n)} - \varepsilon_m\cdot kd\cdot\zeta_1^{(m)}=0 \tag{4}$$

(from (12) of paper I),

$$\sum_{n=0}^{\infty} I\left(\frac{J_{2n+1}}{r},\ m\right)\cdot\zeta_2^{(2n+1)} + i\cdot\varepsilon_m\cdot k_1^{(m)}d\cdot\zeta_1^{(m)}=0 \tag{5}$$

(from (13) of paper I),

$$J_{2m}(kd)\cdot\overline{\zeta}_2^{(2m)} + \frac{1}{\varepsilon_m}\cdot\sum_{n=0}^{\infty}\frac{2}{\pi}\cdot\frac{(2n+1)\cdot J_{2n+1}(kd)}{(2n+1)^2-(2m)^2}\cdot\zeta_2^{(2n+1)}$$

$$= H_{2m}^{(1)}(kd)\cdot\zeta_3^{(2m)} + \frac{1}{\varepsilon_m}\cdot 2J_{2m}(kd)\cdot\zeta_0 \tag{6}$$

(from (14) of paper I),

$$J'_{2m}(kd)\cdot\overline{\zeta}_2^{(2m)} + \frac{1}{\varepsilon_m}\cdot\sum_{n=0}^{\infty}\frac{2}{\pi}\cdot\frac{(2n+1)\cdot J'_{2n+1}(kd)}{(2n+1)^2-(2m)^2}\cdot\zeta_2^{(2n+1)}$$

$$= H_{2m}^{(1)\prime}(kd)\cdot\zeta_3^{(2m)} + \frac{1}{\varepsilon_m}\cdot 2J'_{2m}(kd)\cdot\zeta_0 \tag{7}$$

(from (15) of paper I),

where

$$\left.\begin{aligned} I(J_{2n}, q) &= \int_0^{kd} J_{2n}(z)\cos\frac{q\pi}{kd}z\,dz\,, \\ I\left(\frac{J_{2n+1}}{r}, q\right) &= (2n+1)\int_0^{kd}\frac{J_{2n+1}(z)}{z}\cos\frac{q\pi}{kd}z\,dz\,, \\ &\qquad (n, q=0, 1, 2, \cdots)\,; \end{aligned}\right\} \tag{8}$$

$$\left.\begin{aligned} \varepsilon_m &= 1 \qquad (m=0) \\ &= 1/2 \quad (m\geqq 1) \end{aligned}\right\};$$

and m is a non-negative integer.

3) T. Momoi, *Bull. Earthq. Res. Inst.*, **43** (1965), 269–289.

In the subsequent two sections, the further reductions are made, following the second procedure of the method of the buffer domain, i.e., an expansion of the expressions of the buffer domain by power series.

4. Third Approximation

In this section, general forms without any simplification, which are described in (4)–(7) of Section 3, are further developed under the third approximation such that

$$\left.\begin{aligned} J_0(z) &\simeq 1-\frac{z^2}{2^2}, \\ J_1(z) &\simeq \frac{z}{2}-\frac{z^3}{2^3\cdot 2!}, \\ J_2(z) &\simeq \frac{z^2}{2^2\cdot 2!}, \\ J_3(z) &\simeq \frac{z^3}{2^3\cdot 3!}, \\ J_m(z) &\simeq 0 \qquad (m\geqq 4), \end{aligned}\right\} \text{ for } z\leqq kd. \tag{9}$$

The above approximations denote that the Bessel functions are retained up to the terms of the third order of $(z/2)$.

Substituting (9) into (8) and after a few reductions, we have:—

$$\left.\begin{aligned} I(J_0, 0) &= kd-\frac{1}{12}(kd)^3, \\ I(J_0, q) &= \frac{(-1)^{q+1}}{2}\cdot\frac{(kd)^3}{(q\pi)^2} \qquad (q\geqq 1), \\ I(J_2, 0) &= \frac{1}{24}(kd)^3, \\ I(J_2, q) &= \frac{(-1)^q}{4}\cdot\frac{(kd)^3}{(q\pi)^2} \qquad (q\geqq 1), \\ I(J_{2n}, q) &= 0 \qquad (n\geqq 2,\quad q\geqq 0), \end{aligned}\right\} \tag{10}$$

$$\left.\begin{aligned} I\left(\frac{J_1}{r}, 0\right) &= \frac{1}{2}kd-\frac{1}{48}(kd)^3, \\ I\left(\frac{J_1}{r}, q\right) &= \frac{(-1)^{q+1}}{8}\cdot\frac{(kd)^3}{(q\pi)^2} \qquad (q\geqq 1), \end{aligned}\right\}$$

$$\left.\begin{aligned} &I\left(\frac{J_3}{r},\ 0\right)=\frac{1}{48}(kd)^3, \\ &I\left(\frac{J_3}{r},\ q\right)=\frac{(-1)^q}{8}\cdot\frac{(kd)^3}{(q\pi)^2} \qquad (q\geqq 1), \\ &I\left(\frac{J_{2n+1}}{r},\ q\right)=0 \qquad (n\geqq 2,\ q\geqq 0). \end{aligned}\right\} \tag{11}$$

From (9), the derivatives of the Bessel functions become as follows:—

$$\left.\begin{aligned} &J_0'(z)\simeq -\frac{z}{2}, \\ &J_1'(z)\simeq \frac{1}{2}-\frac{3}{2^3\cdot 2!}z^2, \\ &J_2'(z)\simeq \frac{z}{2\cdot 2!}, \\ &J_3'(z)\simeq \frac{z^2}{2^3\cdot 2!}, \\ &J_m'(z)\simeq 0 \qquad (m\geqq 4), \end{aligned}\right\} \text{ for } z\leqq kd. \tag{12}$$

Putting (9)–(12) into the expressions of the buffer domain D_2 in the infinite simultaneous equations of Section 3, these equations are reduced to:—

$$\sum_{n=0}^{1} I(J_{2n},\ m)\cdot\overline{\zeta}_2^{(2n)}-\varepsilon_m\cdot kd\cdot\zeta_1^{(m)}=0 \qquad (m\geqq 0), \tag{13}$$

$$\sum_{n=0}^{1} I\left(\frac{J_{2n+1}}{r},\ m\right)\cdot\zeta_2^{(2n+1)}+i\cdot\varepsilon_m\cdot k_1^{(m)}d\cdot\zeta_1^{(m)}=0 \qquad (m\geqq 0), \tag{14}$$

$$\left.\begin{aligned} &J_{2m}(kd)\cdot\overline{\zeta}_2^{(2m)}+\frac{1}{\varepsilon_m}\cdot\sum_{n=0}^{1}\frac{2}{\pi}\cdot\frac{(2n+1)\cdot J_{2n+1}(kd)}{(2n+1)^2-(2m)^2}\cdot\zeta_2^{(2n+1)} \\ &\quad -H_{2m}^{(1)}(kd)\cdot\zeta_3^{(2m)}=\frac{2}{\varepsilon_m}\cdot J_{2m}(kd)\cdot\zeta_0 \qquad (m=0,\ 1), \\ &\frac{1}{\varepsilon_m}\cdot\sum_{n=0}^{1}\frac{2}{\pi}\cdot\frac{(2n+1)\cdot J_{2n+1}(kd)}{(2n+1)^2-(2m)^2}\cdot\zeta_2^{(2n+1)}-i\cdot Y_{2m}(kd)\cdot\zeta_3^{(2m)}=0 \\ &\qquad (m\geqq 2), \end{aligned}\right\} \tag{15}$$

$$\left.\begin{aligned} &J'_{2m}(kd)\cdot\zeta_2^{(2m)}+\frac{1}{\varepsilon_m}\cdot\sum_{n=0}^{1}\frac{2}{\pi}\cdot\frac{(2n+1)\cdot J'_{2n+1}(kd)}{(2n+1)^2-(2m)^2}\cdot\zeta_2^{(2n+1)}\\ &\quad -H_{2m}^{(1)\prime}(kd)\cdot\zeta_3^{(2m)}=\frac{2}{\varepsilon_m}\cdot J'_{2m}(kd)\cdot\zeta_0 \qquad (m=0,\ 1),\\ &\frac{1}{\varepsilon_m}\cdot\sum_{n=0}^{1}\frac{2}{\pi}\cdot\frac{(2n+1)\cdot J'_{2n+1}(kd)}{(2n+1)^2-(2m)^2}\cdot\zeta_2^{(2n+1)}-i\cdot Y'_{2m}(kd)\cdot\zeta_3^{(2m)}=0\\ &\qquad (m\geqq 2), \end{aligned}\right\} \tag{16}$$

where

$$\left.\begin{aligned} &I(J_{2n},\ m)\\ &I\left(\frac{J_{2n+1}}{r},\ m\right)\end{aligned}\right\} \qquad (n=0,\ 1;\ m\geqq 0)$$

and

$$\left.\begin{aligned} &J_n(kd)\\ &J'_n(kd)\end{aligned}\right\} \qquad (n=0,\ 1,\ 2,\ 3)$$

have forms described in (9)–(12).

The equations (13)–(16) up to $m=1$ constitute simulateneous equations with eight unknowns:—

$$\zeta_1^{(0)},\ \zeta_1^{(1)},\ \bar{\zeta}_2^{(0)},\ \bar{\zeta}_2^{(2)},\ \zeta_2^{(1)},\ \zeta_2^{(3)},\ \zeta_3^{(0)} \text{ and } \zeta_3^{(2)}. \tag{17}$$

These equations are readily solved with an electronic computer. In actual calculations, the approximate expressions ((9), (12)) of the Bessel functions and their derivatives are not used, for the use of the subroutine of the Bessel functions in a computer makes the calculation of the rigorous forms of the functions easier than their approximate expressions. Then the derivatives of the Bessel functions are computed by

$$Z'_n(z)=nZ_n(z)\cdot z-Z_{n+1}(z), \tag{18}$$

where $Z_n(z)$ stands for $J_n(z)$ or $Y_n(z)$.

Such a convention is followed in the calculations of the fourth and fifth approximations in the subsequent sections.

The significance of the approximate expressions of the Bessel functions (9) is to reduce the infinite simultaneous equations of Section 3 to the finite number of the simultaneous equations. This process is very important in our method (the method of the buffer domain).

After solving the equations (13)–(16) up to $m=1$, we can obtain the numerical values of the unknowns given in (17). Substituting these solu-

tions into (13) and (15) for $m \geqq 2$, the higher modes of the waves $\zeta_1^{(m)}$ and $\zeta_3^{(2m)}$ for $m \geqq 2$ are readily computed. Now, the substitution of the above unknowns $\zeta_1^{(m)}$ and $\zeta_3^{(2m)}$ $(m \geqq 0)$ into the formal solutions (1) and (3) enables us to visualize the variations of the waves in the domains D_1 and D_3 with a help of a computer.

As far as the waves in the domain D_2 are concerned, the formal solution (2) is reduced to

$$\zeta_2 = \sum_{n=0}^{1} \{\zeta_2^{(2n)} \cos 2n\theta \cdot J_{2n}(kr) + \zeta_2^{(2n+1)} \sin (2n+1)\theta \cdot J_{2n+1}(kr)\} \tag{19}$$

(note: the upper limit of $\sum$ is 1 in place of ∞ in (2)), since $J_m(kr)$ $(r \leqq d)$ $m \geqq 4$ can be set down equal to zero from the approximation (9). By use of the solutions obtained in (17) and the above expression (19), the behavior of the waves in front of the canal (in the domain D_2) is readily examined numerically.

The results of the calculations and their discussions are made in later Section 7.

5. Fourth Approximation

In this section, general forms (4)–(7) are further reduced under the approximations such that

$$\left.\begin{aligned} J_0(z) &\simeq 1 - \frac{z^2}{2^2} + \frac{z^4}{2^2 \cdot 4^2}, \\ J_1(z) &\simeq \frac{z}{2} - \frac{z^3}{2^3 \cdot 2!}, \\ J_2(z) &\simeq \frac{z^2}{2^2 \cdot 2!} - \frac{z^4}{2^4 \cdot 1! \cdot 3!}, \\ J_3(z) &\simeq \frac{z^3}{2^3 \cdot 3!}, \\ J_4(z) &\simeq \frac{z^4}{2^4 \cdot 4!}, \\ J_m(z) &\simeq 0 \qquad (m \geqq 5), \end{aligned}\right\} \quad \text{for } z \leqq kd. \tag{20}$$

In the approximations described above, the Bessel functions are retained up to the terms of the fourth order of $(z/2)$.

A substitution of (20) in (8) yields:—

$$
\left.\begin{aligned}
&I(J_0,\,0)=kd-\frac{1}{12}(kd)^3+\frac{1}{320}(kd)^5\,,\\
&I(J_0,\,q)=\frac{(-1)^{q+1}}{2}\cdot\frac{(kd)^3}{(q\pi)^2}+\frac{(-1)^q}{16}\cdot\frac{\{(q\pi)^2-6\}}{(q\pi)^4}\cdot(kd)^5 \qquad (q\geqq 1)\,,\\
&I(J_2,\,0)=\frac{1}{24}(kd)^3-\frac{1}{480}(kd)^5\,,\\
&I(J_2,\,q)=-\frac{(-1)^q}{4}\cdot\frac{(kd)^3}{(q\pi)^2}+\frac{(-1)^{q+1}}{24}\cdot\frac{\{(q\pi)^2-6\}}{(q\pi)^4}\cdot(kd)^5 \qquad (q\geqq 1)\,,\\
&I(J_4,\,0)=\frac{1}{1920}(kd)^5\,,\\
&I(J_4,\,q)=\frac{(-1)^q}{96}\cdot\frac{\{(q\pi)^2-6\}}{(q\pi)^4}\cdot(kd)^5 \qquad (q\geqq 1)\,,\\
&I(J_{2n},\,q)=0 \qquad (n\geqq 3,\ q\geqq 0)\,,
\end{aligned}\right\} \tag{21}
$$

$$
\left.\begin{aligned}
&I\left(\frac{J_{2n+1}}{r}\,,\ q\right) \quad (n\geqq 0\,,\ q\geqq 0)\\
&\text{have completely the same expressions as those given in (11)}\\
&\text{of the previous section (the case of the third approximation).}
\end{aligned}\right\} \tag{22}
$$

From (20), the derivatives of the Bessel functions are given as follows:—

$$
\left.\begin{aligned}
&J_0'(z)\simeq-\frac{z}{2}+\frac{z^3}{2^2\cdot 4}\,,\\
&J_1''(z)\simeq\frac{1}{2}-\frac{3}{2^3\cdot 2!}z^2\,,\\
&J_2'(z)\simeq\frac{z}{2\cdot 2!}-\frac{z^3}{2^2\cdot 1!\cdot 3!}\,,\\
&J_3'(z)\simeq\frac{z^2}{2^3\cdot 2!}\,,\\
&J_4'(z)\simeq\frac{z^3}{2^4\cdot 3!}\,,\\
&J_m'(z)\simeq 0 \qquad (m\geqq 5)\,,
\end{aligned}\right\} \quad \text{for } z\leqq kd\,. \tag{23}
$$

Using the approximated expressions (20)–(23), the infinite simultaneous equations (4)–(7) are reduced to the following:—

$$
\sum_{n=0}^{2} I(J_{2n},\,m)\cdot\overline{\zeta}_2^{(2n)}-\varepsilon_m\cdot kd\cdot\zeta_1^{(m)}=0 \tag{24}
$$

($m \geqq 0$; the upper limit of $\sum$ becomes 2 in place of 1 for the third approximation (refer to (13))),

$$\sum_{n=0}^{1} I\left(\frac{J_{2n+1}}{r},\ m\right)\cdot\zeta_2^{(2n+1)}+i\cdot\varepsilon_m\cdot k_1^{(m)}d\cdot\zeta_1^{(m)}=0 \tag{25}$$

($m \geqq 0$; this expression is exactly the same as that given in the third approximation (refer to (14))),

$$J_{2m}(kd)\cdot\bar{\zeta}_2^{(2m)}+\frac{1}{\varepsilon_m}\cdot\sum_{n=0}^{1}\frac{2}{\pi}\cdot\frac{(2n+1)\cdot J_{2n+1}(kd)}{(2n+1)^2-(2m)^2}\cdot\zeta_2^{(2n+1)}$$
$$-H_{2m}^{(1)}(kd)\cdot\zeta_3^{(2m)}=\frac{2}{\varepsilon_m}\cdot J_{2m}(kd)\cdot\zeta_0 \tag{26}$$

($m=0,\ 1,\ 2$; it is noted here that the parameter m is taken up to 2, though the above expression is equal to the first one given in (15)),

$$\frac{1}{\varepsilon_m}\cdot\sum_{n=0}^{1}\frac{2}{\pi}\cdot\frac{(2n+1)\cdot J_{2n+1}(kd)}{(2n+1)^2-(2m)^2}\cdot\zeta_2^{(2n+1)}-i\cdot Y_{2m}(kd)\cdot\zeta_3^{(2m)}=0 \tag{26'}$$

($m \geqq 3$; the above expression is the same as the second one in (15) except that $m \geqq 3$ instead of $m \geqq 2$ for (15); the equations (26) and (26′) are derived from (6)),

$$J'_{2m}(kd)\cdot\bar{\zeta}_2^{(2m)}+\frac{1}{\varepsilon_m}\cdot\sum_{n=0}^{1}\frac{2}{\pi}\cdot\frac{(2n+1)\cdot J'_{2n+1}(kd)}{(2n+1)^2-(2m)^2}\cdot\zeta_2^{(2n+1)}$$
$$-H_{2m}^{(1)\prime}(kd)\cdot\zeta_3^{(2m)}=\frac{2}{\varepsilon_m}\cdot J'_{2m}(kd)\cdot\zeta_0 \tag{27}$$

($m=0,\ 1,\ 2$; in the above equation, m is taken up to 2 instead of 1 (refer to the first equation given in (16))),

$$\frac{1}{\varepsilon_m}\cdot\sum_{n=0}^{1}\frac{2}{\pi}\cdot\frac{(2n+1)\cdot J'_{2n+1}(kd)}{(2n+1)^2-(2m)^2}\cdot\zeta_2^{(2n+1)}-i\cdot Y'_{2m}(kd)\cdot\zeta_3^{(2m)}=0 \tag{27'}$$

($m \geqq 3$; in the above expression, $m \geqq 3$ other than $m \geqq 2$ for the case of the third approximation (refer to the second equation of (16)); the equations (27) and (27′) are obtained from (7)),

where

$$\left.\begin{array}{ll} I(J_{2n},\ m) & (n=0,\ 1,\ 2) \\ I\left(\dfrac{J_{2n+1}}{r},\ m\right) & (n=0.\ 1) \end{array}\right\}\ (m\geqq 0)$$

and

$$\left.\begin{array}{l} J_n(kd) \\ J_n'(kd) \end{array}\right\}\ (n=0,\ 1,\ \cdots,\ 4)$$

have already been described in (20)-(23).

Now, we can obtain

$$\zeta_1^{(0)},\ \zeta_1^{(1)},\ \zeta_1^{(2)},\ \overline{\zeta}_2^{(0)},\ \overline{\zeta}_2^{(2)},\ \overline{\zeta}_2^{(4)},\ \zeta_2^{(1)},\ \zeta_2^{(3)},\ \zeta_3^{(0)},\ \zeta_3^{(2)} \text{ and } \zeta_3^{(4)} \tag{28}$$

as solutions of the simultaneous equations which consist of (24) ($m\leqq 2$), (25) ($m\leqq 1$), (26) ($m\leqq 2$) and (27) ($m\leqq 2$).

Substituting $\overline{\zeta}_2^{(2n)}$ ($n=0,\ 1,\ 2$) and $\zeta_2^{(2n+1)}$ ($n=0,\ 1$) solved in the above to (24) and (26′) respectively, the higher modes, $\zeta_1^{(m)}$ and $\zeta_3^{(2m)}$ ($m\geqq 3$), of the waves in the domains D_1 and D_3 are readily computed. Now, using the above obtained $\zeta_1^{(m)}$ and $\zeta_3^{(2m)}$ ($m\geqq 0$), the waves in the parts of the canal and the open sea are elucidated numerically through the expressions (1) and (3).

Since our consideration is limited in the range of the approximation (20), the formal solution (2) describing the waves in the domain D_2 becomes as follows:

$$\zeta_2=\sum_{n=0}^{2}\overline{\zeta}_2^{(2n)}\cos 2n\theta\cdot J_{2n}(kr)+\sum_{n=0}^{1}\zeta_2^{(2n+1)}\sin(2n+1)\theta\cdot J_{2n+1}(kr)\,. \tag{29}$$

In a similar manner to that in the previous section, the behavior of the waves in the domain D_2 is examined numerically by substituting the solutions $\overline{\zeta}_2^{(2n)}$ ($n\leqq 2$) and $\zeta_2^{(2n+1)}$ ($n\leqq 1$) into (29).

The results of the calculations are given in Section 7.

6. Fifth Approximation

In this section, the following approximations are utilized to reduce the infinite simultaneous equations (1)-(7):—

$$\left.\begin{aligned}
J_0(z) &\simeq 1-\frac{z^2}{2^2}+\frac{z^4}{2^2\cdot 4^2}\,,\\
J_1(z) &\simeq \frac{z}{2}-\frac{z^3}{2^3\cdot 1!\cdot 2!}+\frac{z^5}{2^5\cdot 2!\cdot 3!}\,,\\
J_2(z) &\simeq \frac{z^2}{2^2\cdot 2!}-\frac{z^4}{2^4\cdot 1!\cdot 3!}\,,\\
J_3(z) &\simeq \frac{z^3}{2^3\cdot 3!}-\frac{z^5}{2^5\cdot 4!}\,,\\
J_4(z) &\simeq \frac{z^4}{2^4\cdot 4!}\,,\\
J_5(z) &\simeq \frac{z^5}{2^5\cdot 5!}\,,\\
J_m(z) &\simeq 0 \qquad (m\geqq 6)\,,
\end{aligned}\right\} \text{ for } z\leqq kd\,. \tag{30}$$

Then the expressions (8) become, after a few reductions, as follows:—

$$\left.\begin{aligned}
&I(J_{2n},\ q) \quad (n\geqq 0\,,\ q\geqq 0)\\
&\text{have identically the same expressions as}\\
&\text{those given in (21) of Section 5,}
\end{aligned}\right\} \tag{31}$$

$$\left.\begin{aligned}
I\Big(\frac{J_1}{r},\ 0\Big) &= \frac{1}{2}kd-\frac{1}{48}(kd)^3+\frac{1}{1920}(kd)^5\,,\\
I\Big(\frac{J_1}{r},\ q\Big) &= \frac{(-1)^{q+1}}{8}\cdot\frac{(kd)^3}{(q\pi)^2}+\frac{(-1)^q}{96}\cdot\frac{\{(q\pi)^2-6\}}{(q\pi)^4}\cdot(kd)^5 \qquad (q\geqq 1)\,,\\
I\Big(\frac{J_3}{r},\ 0\Big) &= \frac{1}{48}(kd)^3-\frac{1}{1280}(kd)^5\,,\\
I\Big(\frac{J_3}{r},\ q\Big) &= \frac{(-1)^q}{8}\cdot\frac{(kd)^3}{(q\pi)^2}+\frac{(-1)^{q+1}}{64}\cdot\frac{\{(q\pi)^2-6\}}{(q\pi)^4}\cdot(kd)^5 \quad (q\geqq 1)\,,\\
I\Big(\frac{J_5}{r},\ 0\Big) &= \frac{1}{3840}(kd)^5\,,\\
I\Big(\frac{J_5}{r},\ q\Big) &= \frac{(-1)^q}{192}\cdot\frac{\{(q\pi)^2-6\}}{(q\pi)^4}\cdot(kd)^5 \qquad (q\geqq 1)\,,\\
I\Big(\frac{J_{2n+1}}{r},\ q\Big) &= 0 \qquad (n\geqq 3\,,\ q\geqq 0)\,.
\end{aligned}\right\} \tag{32}$$

The Bessel functions (30) yield the derivatives as given below:—

$$\left.\begin{aligned}
&J_0'(z)\simeq -\frac{z}{2}+\frac{z^3}{2^2\cdot 4}\,,\\
&J_1'(z)\simeq \frac{1}{2}-\frac{3}{2^3\cdot 2!}z^2+\frac{5}{2^5\cdot 2!\cdot 3!}z^4\,,\\
&J_2'(z)\simeq \frac{z}{2\cdot 2!}-\frac{z^3}{2^2\cdot 1!\cdot 3!}\,,\\
&J_3'(z)\simeq \frac{z^2}{2^3\cdot 2!}-\frac{5}{2^5\cdot 4!}z^4\,,\\
&J_4'(z)\simeq \frac{z^3}{2^4\cdot 3!}\,,\\
&J_5'(z)\simeq \frac{z^4}{2^5\cdot 4!}\,,\\
&J_m'(z)\simeq 0 \qquad (m\geqq 6)\,,
\end{aligned}\right\} \text{ for } z\leqq kd\,. \tag{33}$$

Substituting the approximated expressions into the infinite simultaneous equations (4)–(7), these equations are reduced to the following ones:—

$$\sum_{n=0}^{2} I(J_{2n},\, m)\cdot\bar{\zeta}_2^{(2n)}-\varepsilon_m\cdot kd\cdot\zeta_1^{(m)}=0 \tag{34}$$

($m\geqq 0$; this equation is the same as that described in (24)),

$$\sum_{n=0}^{2} I\left(\frac{J_{2n+1}}{r},\; m\right)\cdot\zeta_2^{(2n+1)}+i\cdot\varepsilon_m\cdot k_1^{(m)}d\cdot\zeta_1^{(m)}=0 \tag{35}$$

($m\geqq 0$; this expression is the same as that given in (25) except that the upper limit of $\sum$ is 2 instead of 1),

$$\begin{aligned}
&J_{2m}(kd)\cdot\bar{\zeta}_2^{(2m)}+\frac{1}{\varepsilon_m}\cdot\sum_{n=0}^{2}\frac{2}{\pi}\cdot\frac{(2n+1)\cdot J_{2n+1}(kd)}{(2n+1)^2-(2m)^2}\cdot\zeta_2^{(2n+1)}\\
&-H_{2m}^{(1)}(kd)\cdot\zeta_3^{(2m)}=\frac{2}{\varepsilon_m}J_{2m}(kd)\cdot\zeta_0
\end{aligned} \tag{36}$$

($m=0,\ 1,\ 2$; the above equation is the same as that given in (26) except that the upper limit of $\sum$ is 2 in place of 1),

$$\frac{1}{\varepsilon_m}\cdot\sum_{n=0}^{2}\frac{2}{\pi}\cdot\frac{(2n+1)\cdot J_{2n+1}(kd)}{(2n+1)^2-(2m)^2}\cdot\zeta_2^{(2n+1)}-i\cdot Y_{2m}(kd)\cdot\zeta_3^{(2m)}=0 \tag{36'}$$

($m\geqq 3$; the upper limit of $\sum$ in the above equation is 2, though that in (26′) is 1),

$$J'_{2m}(kd)\cdot\overline{\zeta}_2^{(2m)}+\frac{1}{\varepsilon_m}\cdot\sum_{n=0}^{2}\frac{2}{\pi}\cdot\frac{(2n+1)\cdot J'_{2n+1}(kd)}{(2n+1)^2-(2m)^2}\cdot\zeta_2^{(2n+1)}$$

$$-H_{2m}^{(1)\prime}(kd)\cdot\zeta_3^{(2m)}=\frac{2}{\varepsilon_m}\cdot J'_{2m}(kd)\cdot\zeta_0 \tag{37}$$

($m=0,\ 1,\ 2$; except that the upper limit of $\sum$ is 2, the above equation is the same as that expressed in (27)),

$$\frac{1}{\varepsilon_m}\cdot\sum_{n=0}^{2}\frac{2}{\pi}\cdot\frac{(2n+1)\cdot J'_{2n+1}(kd)}{(2n+1)^2-(2m)^2}\cdot\zeta_2^{(2n+1)}-i\cdot Y'_{2m}(kd)\cdot\zeta_3^{(2m)}=0 \tag{37'}$$

($m\geqq 3$; except for a difference of the upper limit of $\sum$, the above expression is the same as that given in (27′)),

where

$$\left.\begin{matrix} I(J_{2n},\ m) \\ I\left(\dfrac{J_{2n+1}}{r},\ m\right)\end{matrix}\right\}\ (n=0,\ 1,\ 2;\ m\geqq 0)$$

and

$$\left.\begin{matrix} J_n(kd) \\ J'_n(kd)\end{matrix}\right\}\ (n=0,\ 1,\ \cdots,\ 5)$$

have already been given in (30)–(33).

In a manner similar to the procedures given in Sections 4 and 5, the unknowns

$$\zeta_1^{(0)},\ \zeta_1^{(1)},\ \zeta_1^{(2)},\ \overline{\zeta}_2^{(0)},\ \overline{\zeta}_2^{(2)},\ \overline{\zeta}_2^{(4)},\ \zeta_2^{(1)},\ \zeta_2^{(3)},\ \zeta_2^{(5)},\ \zeta_3^{(0)},\ \zeta_3^{(2)}\ \text{and}\ \zeta_3^{(4)} \tag{38}$$

are obtained as solutions of the simultaneous equations (34), (35), (36) and (37) for $m=0,\ 1,\ 2$. Then a substitution of (38) into (34) ($m\geqq 3$) and (36′) gives higher modes $\zeta_1^{(m)}$ and $\zeta_3^{(2m)}$ for $m\geqq 3$, which enables us to elucidate numerically the behavior of the waves in the parts of the canal and the open sea through the expressions (1) and (3).

In the present approximation, the formal solution (2) becomes as follows:—

$$\zeta_2=\sum_{n=0}^{2}\{\overline{\zeta}_2^{(2n)}\cos 2n\theta\cdot J_{2n}(kr)+\zeta_2^{(2n+1)}\sin(2n+1)\theta\cdot J_{2n+1}(kr)\} \tag{39}$$

By substitution of the solutions (38) into (39), we can determine the variation of the waves in front of the mouth of the canal.

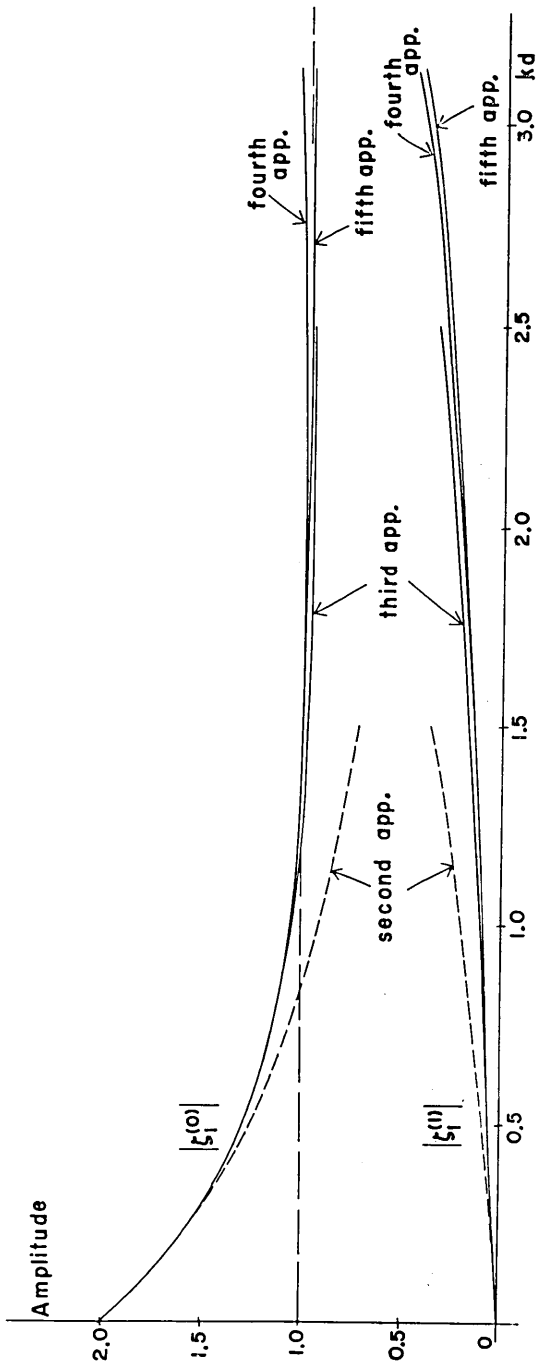

Fig. 2. Variations of the amplitudes $|\zeta_1^{(0)}|$ and $|\zeta_1^{(1)}|$ for change of kd.

The results of the numerical calculations are given in the subsequent section.

7. Numerical Results and Discussions

In this section, the theories developed under the approximations of the third (in Section 4), fourth (in Section 5) and fifth (in Section 6) order of kd are utilized to inquire into the behaviors of the waves around an estuary with the aid of an electronic computer.

To begin with, the waves in the part of the canal are discussed.

The variations of the amplitudes of the advancing mode ($|\zeta_1^{(0)}|$) and the first mode of the damping waves ($|\zeta_1^{(1)}|$) are shown in Fig. 2. In this figure, the broken lines stated by the characters "second app." stand for the curves obtained under the second approximation in paper II, while the solid lines stated by "third app.", "fourth app." and "fifth app." denote the results under the approximations of Sections 4, 5, and 6 in the present work respectively. According to this figure, when the approximation proceeds from the second to the higher ones, the curve $|\zeta_1^{(0)}|$ is upheaved gradually to converge on a certain curve which, when kd increases, runs so as to make a line *Amplitude*$=1.0$ its asymptote. At any rate, as we estimated in paper I, the advancing wave $|\zeta_1^{(0)}|$ (higher modes are damping waves, since our consideration is limited to the range $kd<\pi$) becomes approximately a unit at $kd=1.0$. In other words, the shape of an estuary does not affect the influence upon the advancing waves when $kd=1.0$. As far as the first mode $|\zeta_1^{(1)}|$ is concerned, when the approximation is more generalized, the curve of the first mode begins to be suppressed with a tendency of convergence. The converging line is nearly a straight one which has the origin at $kd=0$ and amounts to about 0.4 at $kd=\pi$.

We consider next the phases of the waves in the canal. As described in (56)–(59) of paper II, $\arg\zeta_1^{(0)}$ denotes the phase lag of the waves advancing into the canal and β $(=(\arg\zeta_1^{(0)})/kd)$ the hypothetical origin of the $\cos(\omega t+ky)$-type wave in the expression such that

$$\left.\begin{aligned}\zeta_1&=|\zeta_1^{(0)}|\cos(\omega t+ky-\arg\zeta_1^{(0)})+\zeta_1^{(\mathrm{dam})}\\ \text{or}\quad&=|\zeta_1^{(0)}|\cos\{\omega t+kd(y/d-\beta)\}+\zeta_1^{(\mathrm{dam})}\end{aligned}\right\}, \tag{40}$$

where $\zeta_1^{(\mathrm{dam})}$ is the waves damping towards the canal. The variation of $\arg\zeta_1^{(0)}$ is drawn in Fig. 3, in which the broken line stands for curve based on the theory of the second approximation (in paper II) and the full lines

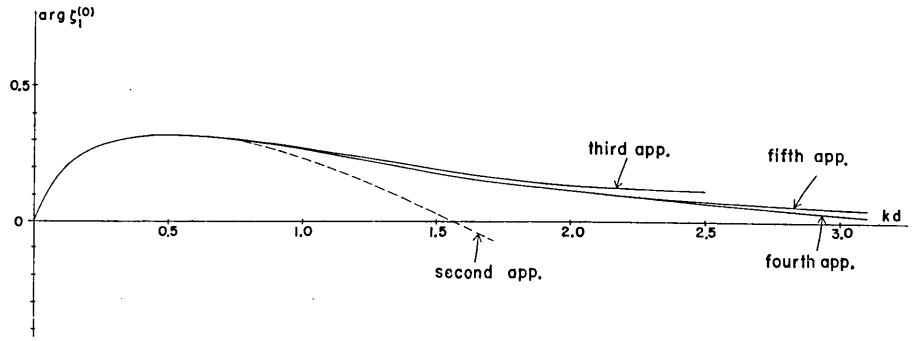

Fig. 3. A variation of the phase of the advancing mode in the canal versus kd.

those for the third, fourth and fifth approximations in the present work. With a generalization of the approximation, a curve of arg $\zeta_1^{(0)}$ is in a sense of convergence. A maximum point which has already been noted in paper II takes place at $kd \simeq 0.5$ and, on the upper side of this point, the curve decreases gradually to tend to the kd-axis without intersection (kd-axis seems to be the asymptote of the curve of arg $\zeta_1^{(0)}$), while, in the stages of the previous approximations (papers I and II), the curve of arg $\zeta_1^{(0)}$ crosses the kd-axis. With regard to the occurrence of the maximum, a physical interpretation has been described in paper II. The curve of β-value is shown in Fig. 4 (the broken line is that for the second approximation in paper II and the solid lines for the approximations in the present work). According to this figure, the curve of β-value converges to a

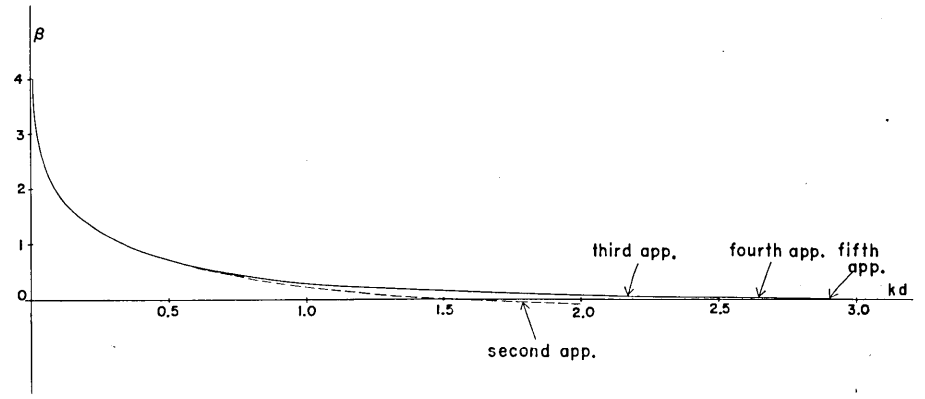

Fig. 4. A variation of a supposed origin of the cos $(\omega t + ky)$-type wave in the canal versus kd.

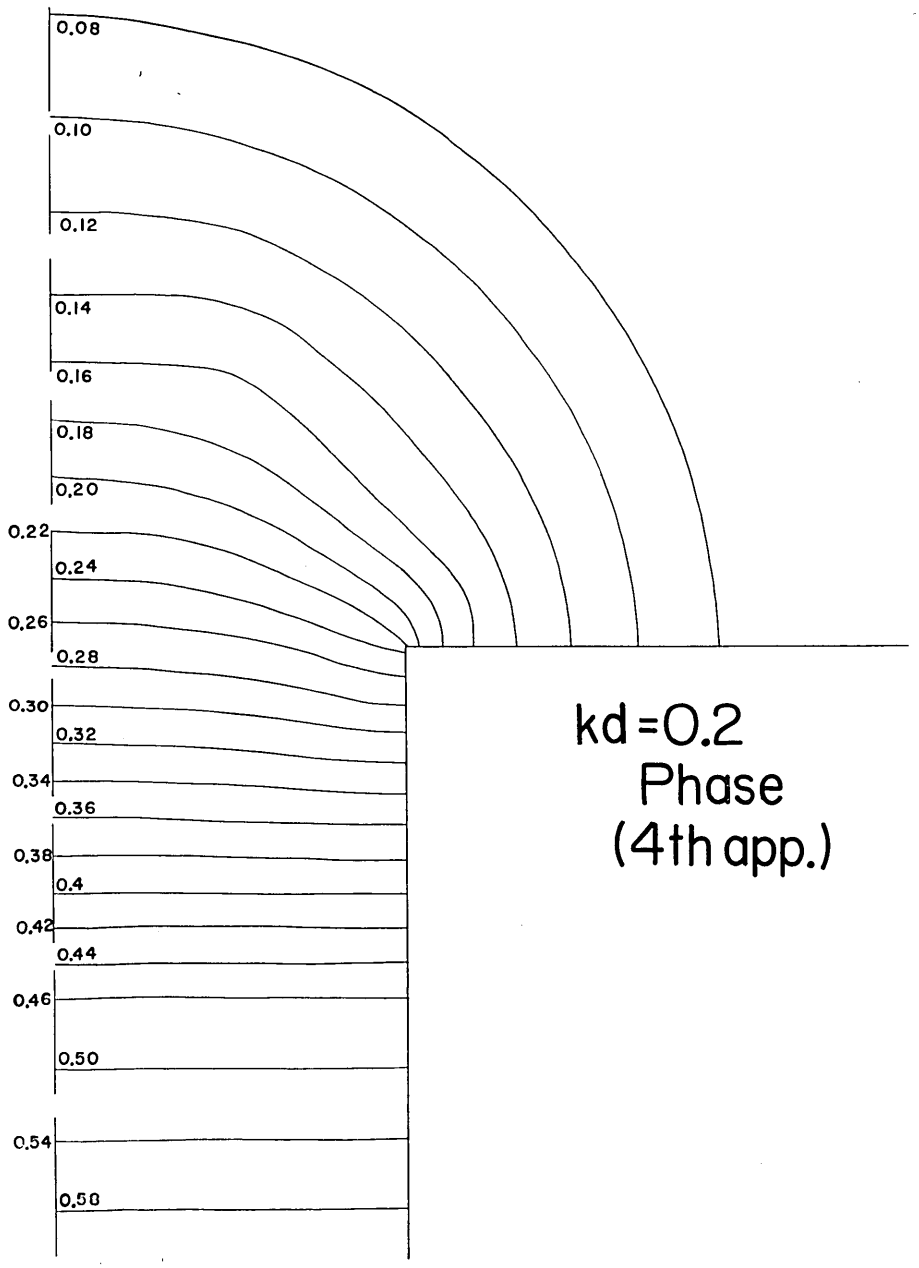

Fig. 5. Isolines of phase around an estuary for kd=0.2 (the stated values stand for arg ζ).

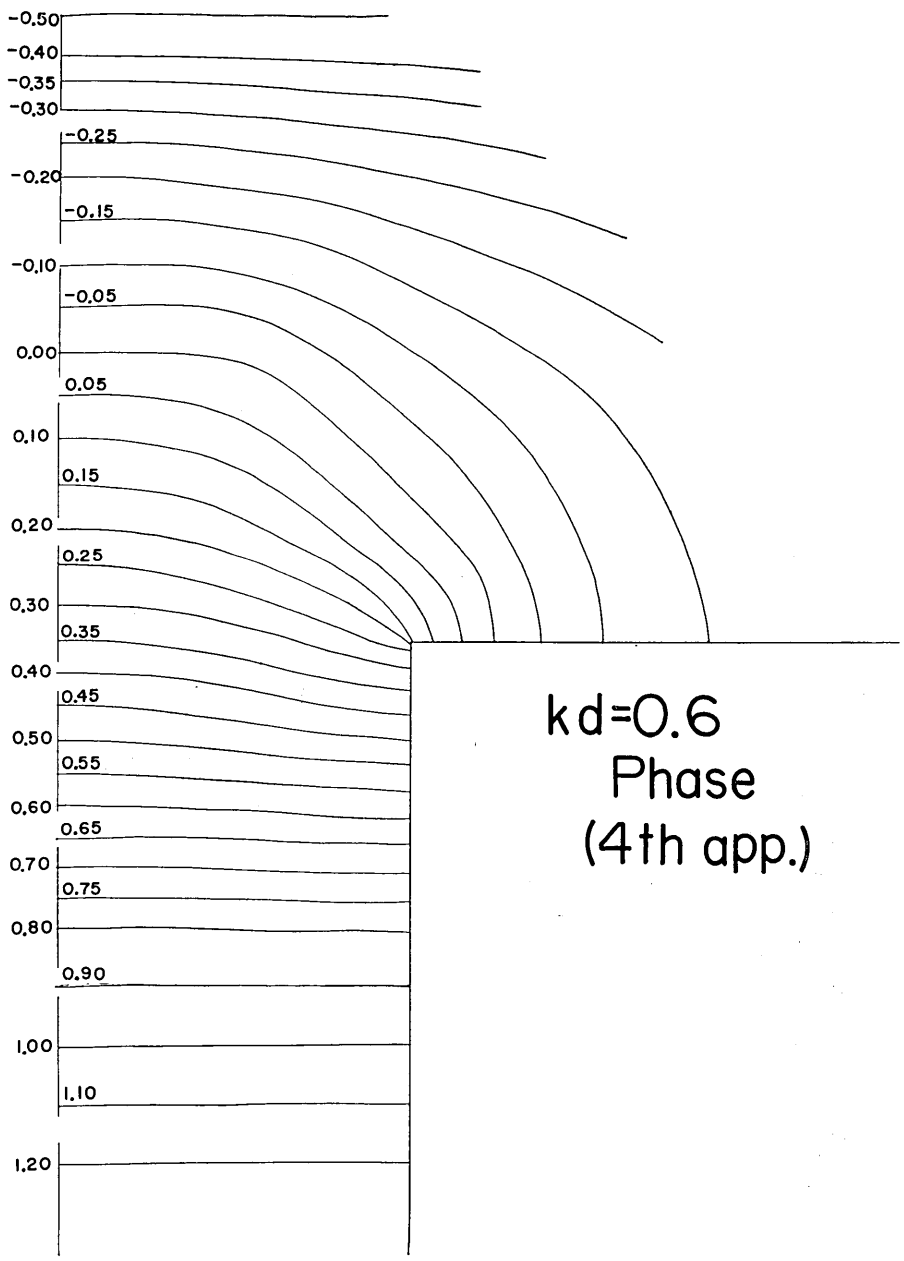

Fig. 6. Isolines of phase around an estuary for kd=0.6 (the stated values stand for arg ζ).

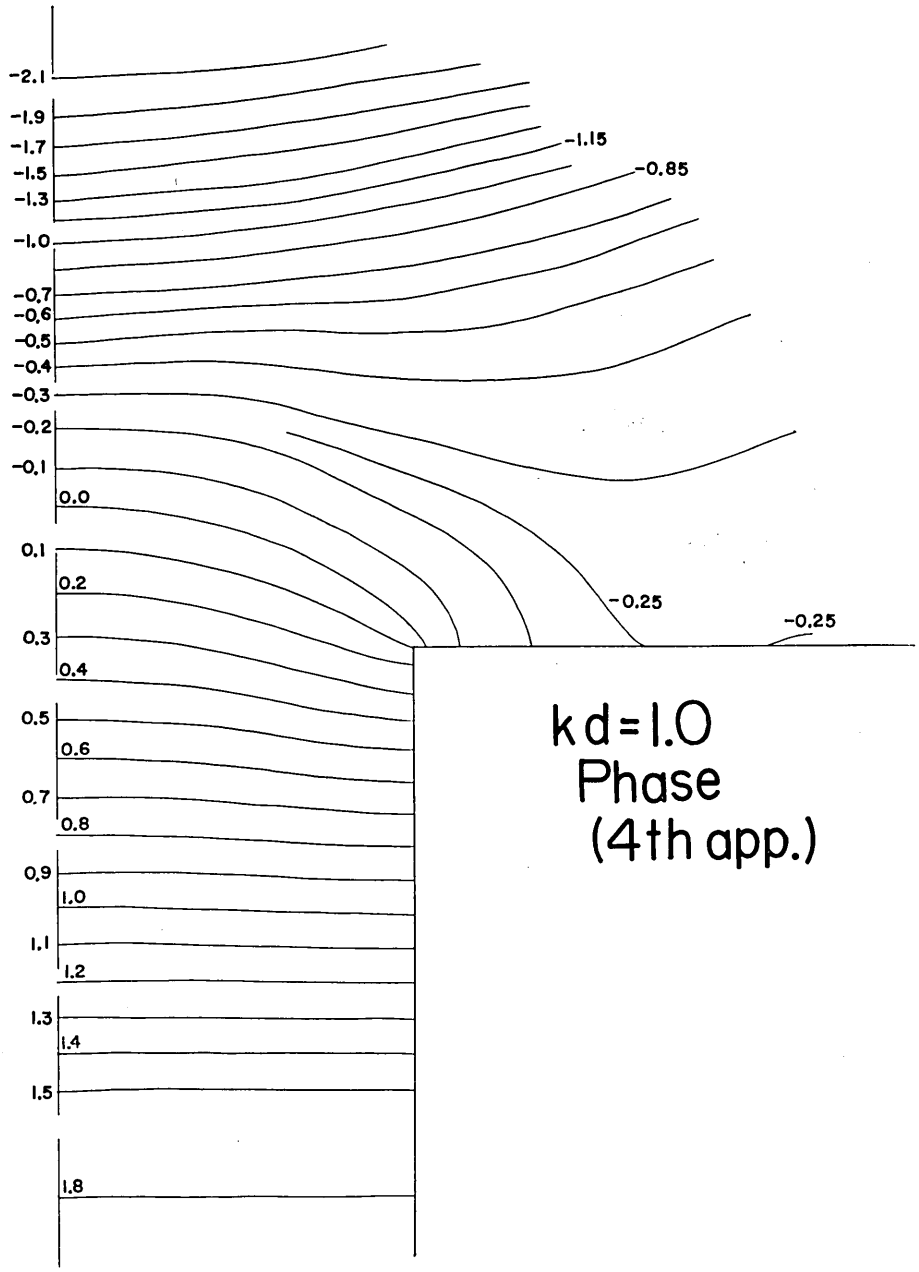

Fig. 7. Isolines of phase around an estuary for kd=1.0 (the stated values stand for arg ζ).

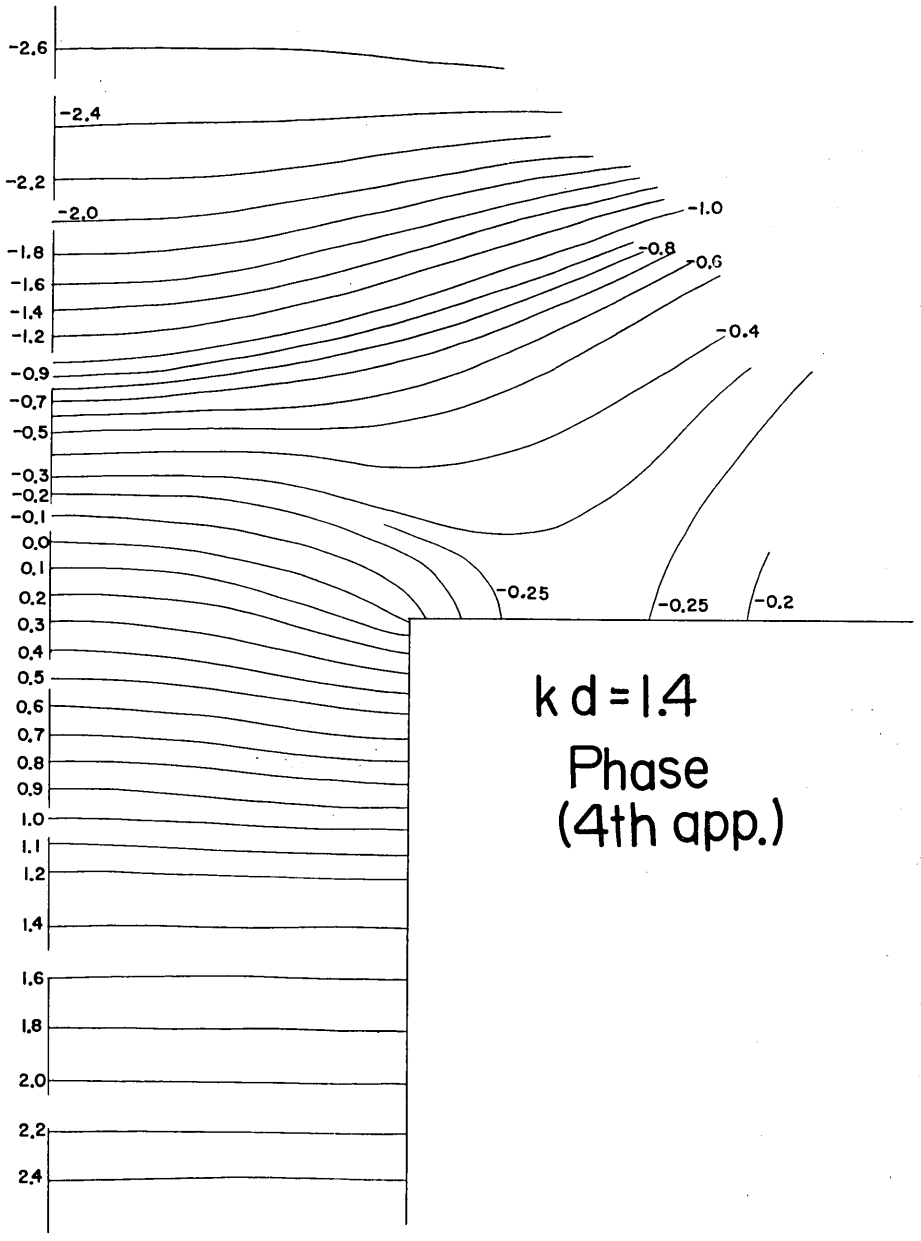

Fig. 8. Isolines of phase around an estuary for kd=1.4 (the stated values stand for arg ζ).

certain curve which has the kd-axis as the asymptote. The supposed origin of the $\cos(\omega t + ky)$-type wave is located at an infinity in the open sea, when kd is very small, (which has already been noted in paper II) and begins to approach infinitely an estuary without crossing, as kd increases.

Next, the overall pictures of the variations of phases and amplitudes of waves are given in Figs. 5 to 8 (for phases) and Figs. 10 to 13 (for amplitudes), which have been drawn for specified values of $kd=0.2$, 0.6, 1.0 and 1.4 on the basis of the theory of the fourth approximation. For the check of convergence, the figures of phases and amplitudes obtained from the theory of the third approximation are shown in Figs. 15 and 16 respectively.

To begin with, the variations of the phases are discussed (Figs. 5 to 8). In the domain D_1 (the part of the canal), the convergence of the waves to the axis of the canal are seen which produces high waves in the interior of the canal (this fact has already been noted in paper II). Passing through all the figures of the part of the canal in Figs. 5 to 8, the rates of convergence of the waves are hardly altered for the range of $kd=0.2$ to 1.4. In the domain D_2 (the region in front of the canal, i.e. buffer domain), the invading waves converge, as a general trend, to the center of the mouth of the canal, but the states of the convergence are different from each other for a change of kd. When kd is augmented, the contours of the isolines of phases vary from an equilateral triangular form (see Fig. 11 in paper II referred to $kd=0.02$) to a trapezoid form (Figs. 5 and 6 referred to $kd=0.2$ and 0.6) which, when kd amounts to 1.4, becomes a very flat form (Fig. 8). These behaviors are illustrated schematically in Fig. 9. Comparing Fig. 8 (the fourth approximation) with Fig. 15 (the third approximation), the extent of convergence of calculated results is fairly good for the above-mentioned discussion. In Fig. 13 of paper II (relevant to $kd=0.5$), such a feature of trapezoid does not appear, the reason for which might be attributed to a deficiency of the approximation (the second approximation). In the domain D_3 (the region of the open sea except a semi-circular area in front of the canal), the waves, for the range of $kd=0.2$ (Fig. 5) to 0.6 (Fig. 6), converge to an estuary in a circular form, while when kd increases further from 0.6 to 1.0, the nature of convergence disappears gradually (Fig. 7) and even divergence behaviors are preferably seen. When kd reaches 1.4 (Fig. 8), such a divergence of waves is found clearly and the diverted waves advance along the straight coast facing the open sea, departing from an estuary.

Referring to Fig. 15 written based on the theory of the third approximation, the divergence of the waves is also seen so that an appearance of the diverted waves around an estuary is considered to be an established fact beyond the error of the approximation.

Next, let us discuss the variations of the amplitudes referring to Figs. 10 to 13. In the domain D_1, a mount and valley appear in the middle and

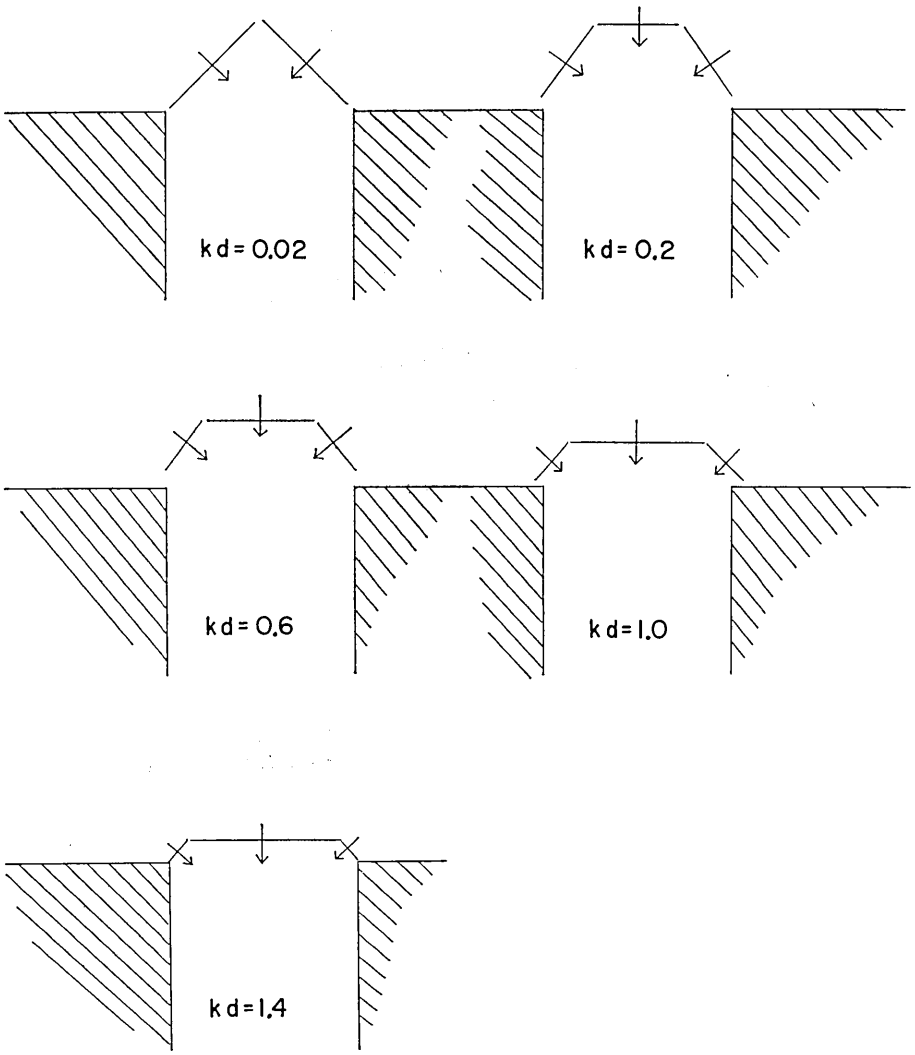

Fig. 9. A variation of forms of crest lines versus kd (arrows stand for the direction of propagation of waves).

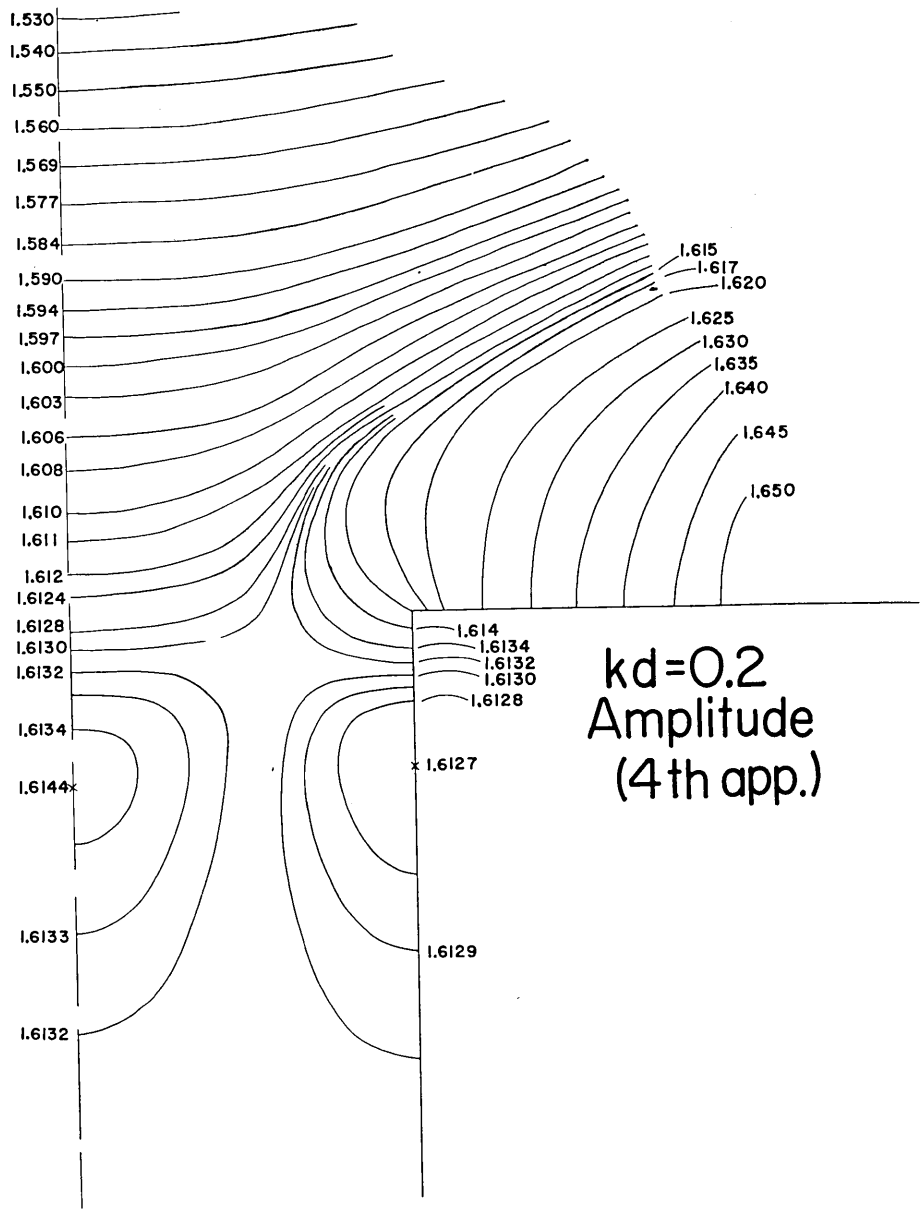

Fig. 10. A variation of amplitude of waves around an estuary for kd=0.2 (the stated values stand for $|\zeta|$).

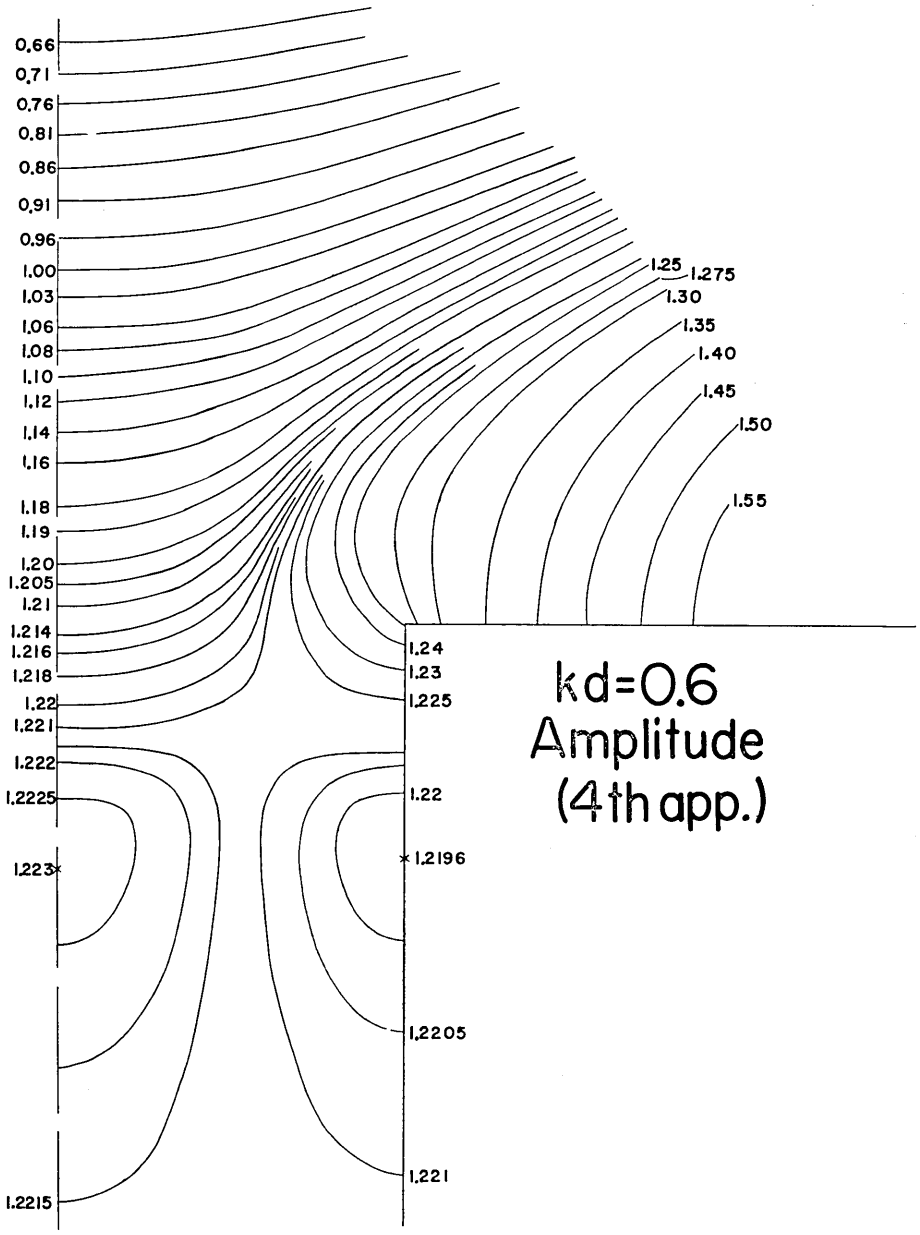

Fig. 11. A variation of amplitude of waves around an estuary for kd=0.6 (the stated values stand for $|\zeta|$).

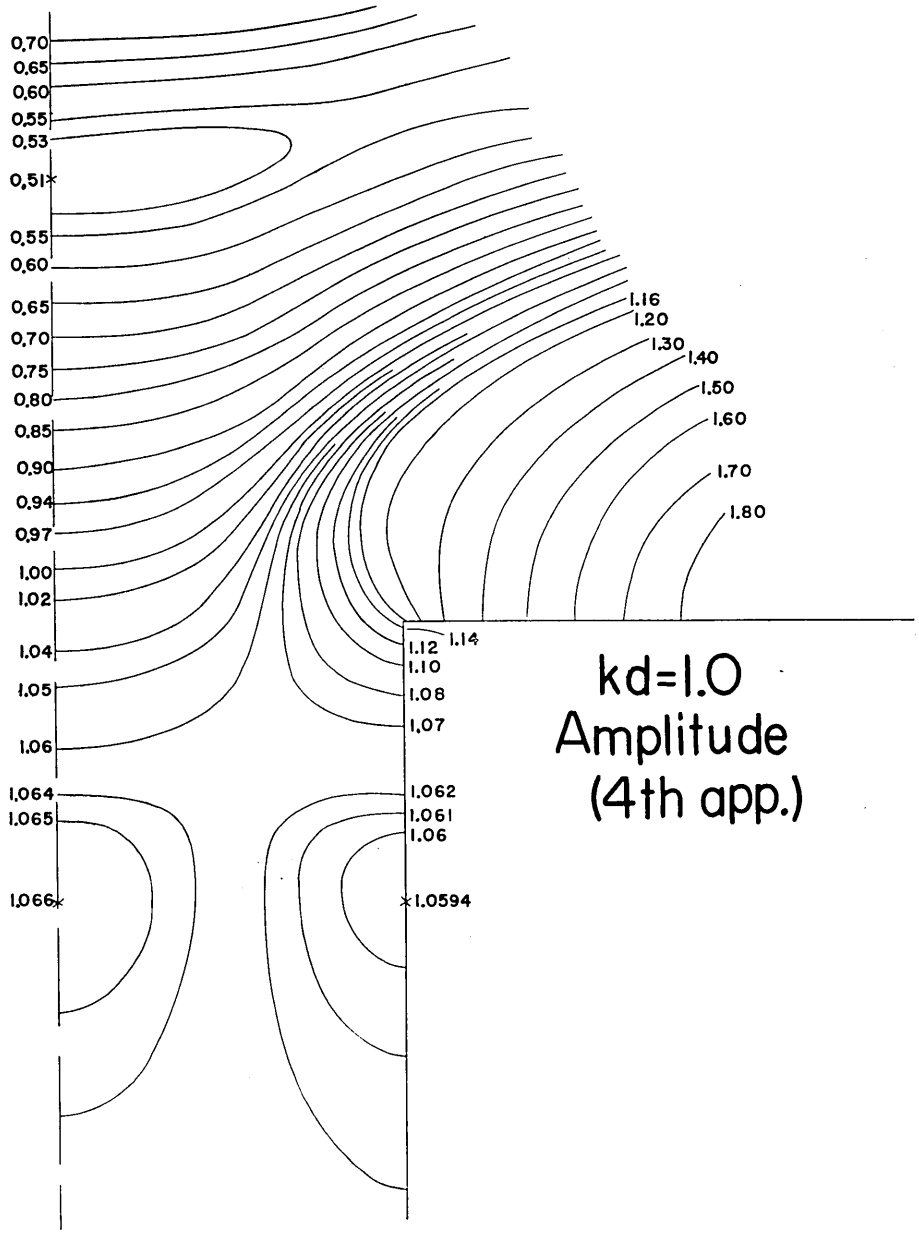

Fig. 12. A variation of amplitude of waves around an estuary for kd=1.0 (the stated values stand for $|\zeta|$).

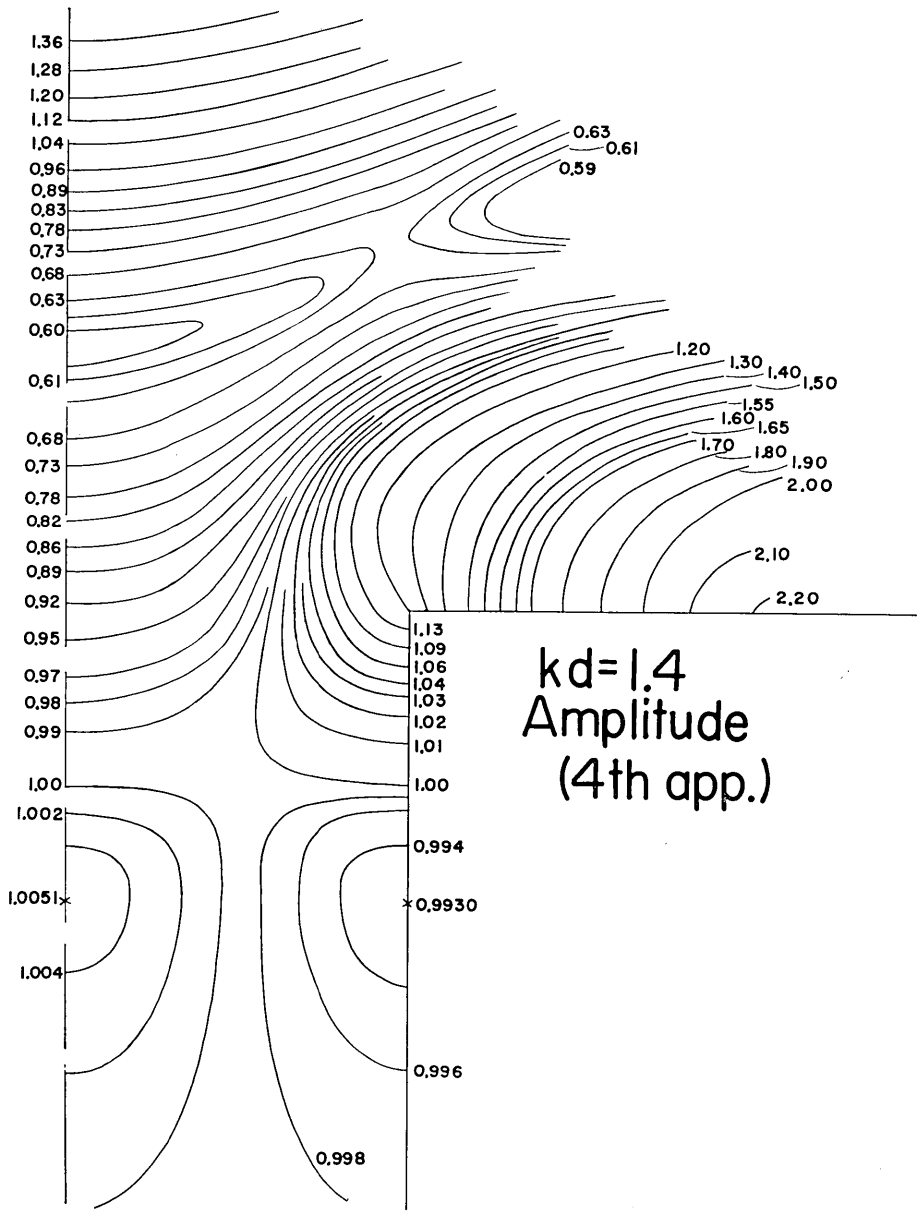

Fig. 13. A variation of amplitude of waves around an estuary for kd=1.4 (the stated values stand for $|\zeta|$).

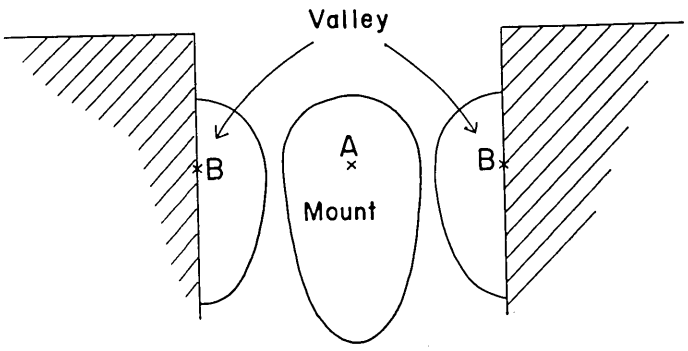

Fig. 14. Explanation of *A* and *B* points.

along the wall of the canal. This mount and valley are interpreted to be caused by an interference of the waves invading directly from the open sea and the waves diffracted around an estuary. The former (a mount) has already been noted in paper II, while the latter (a valley) is passed unnoticed. The differences of the amplitudes at the highest point (A point in Fig. 14) of the mount and at the lowest one (B point in Fig. 14) of the valley are computed, of which the result is arranged in Table 1.

Table 1. Differences of the amplitudes at A and B points (refer to Fig. 14)

kd	$\|\zeta\|_A$	$\|\zeta\|_B$	$\|\zeta\|_A - \|\zeta\|_B$
0.2	1.6144	1.6127	0.0017
0.6	1.2230	1.2196	0.0034
1.0	1.0660	1.0594	0.0066
1.4	1.0051	0.9930	0.0121
(1.4)	(1.0015)	(0.9905)	(0.0110)

where $|\zeta|_A$: amplitude at A point, $|\zeta|_B$: amplitude at B point and the values in the parentheses denote those obtained from Fig. 16 (the figure of the third approximation).

For convergence check, the values obtained from Fig. 16 (the figure of the third approximation) are also listed in Table 1. According to this table, the difference of the amplitudes at the mount and valley is in a sense increasing as kd increases. One more features is seen in the be-

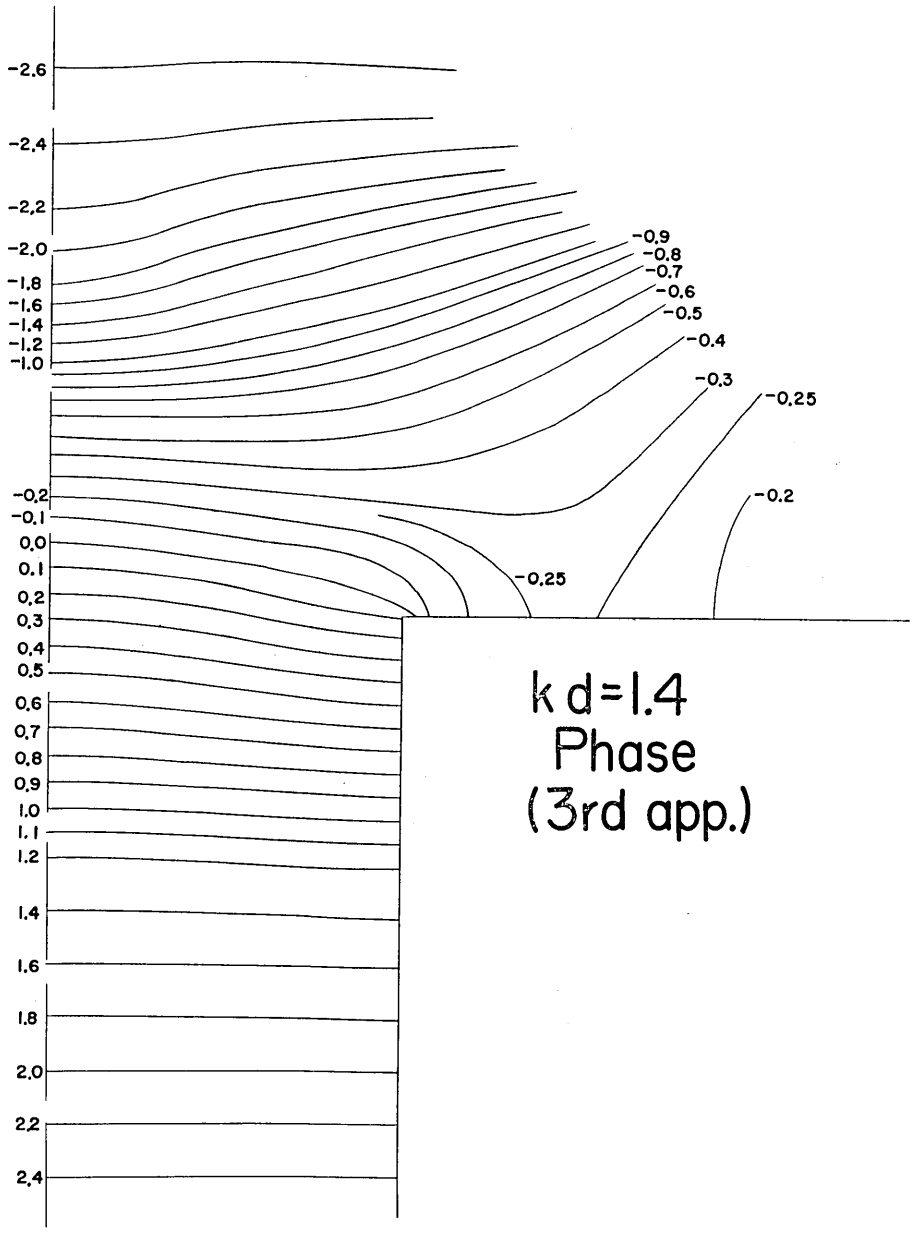

Fig. 15. A variation of phase around an estuary for $kd=1.4$ (the stated values stand for arg ζ, which are computed by the theory of the third approximation).

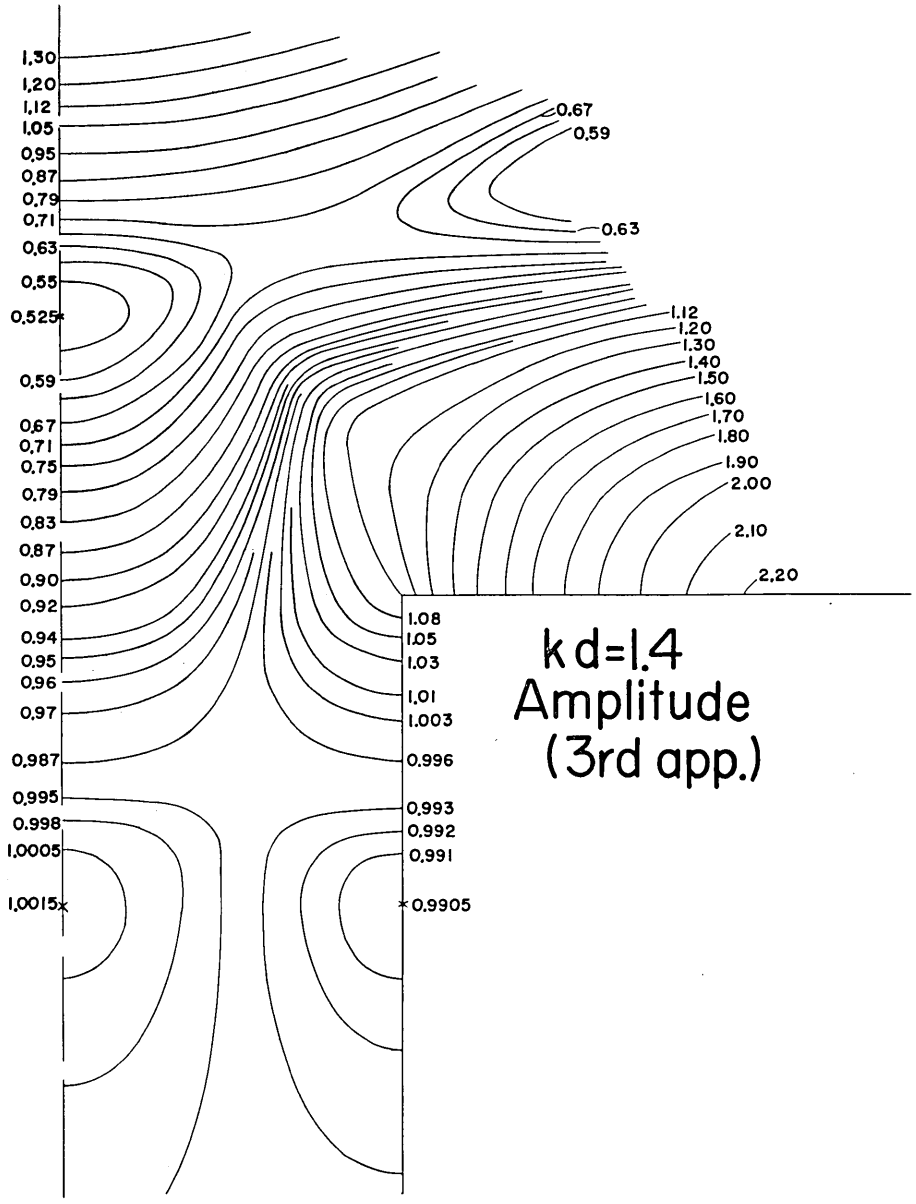

Fig. 16. A variation of amplitude around an estuary for kd=1.4 (the stated values stand for $|\zeta|$, which are computed by the theory of the third approximation).

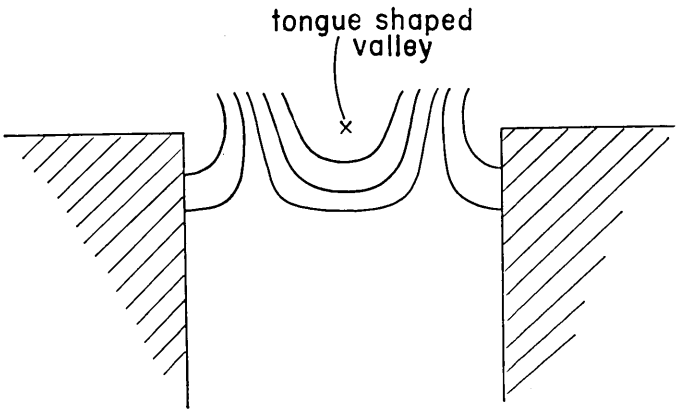

Fig. 17. A figurative explanation of tongue-shaped valley.

haviors of the waves in the canal, that is to say, tongue-shaped valleys are seen to extend to the inside of the canal from the open sea (Fig. 17). Passing through the figures of the amplitude (Figs. 10 to 13), such an extension is found to begin to be greater with an increase of kd. Discussions in the region of the open sea are made through two domains D_2 and D_3.

Referring to Figs. 10 to 13, the isolines of the amplitude in the open sea bend down to the direction of a canal. For the figures of $kd=0.2$ and 0.6 (Figs. 10 and 11), the amplitude is increasing monotonically in magni-

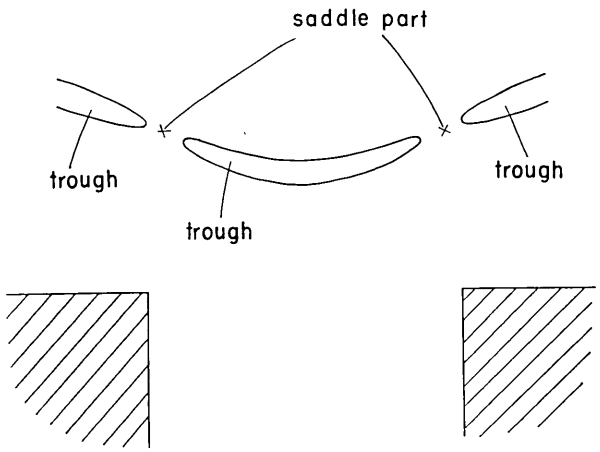

Fig. 18. Figurative explanations of trough and saddle part.

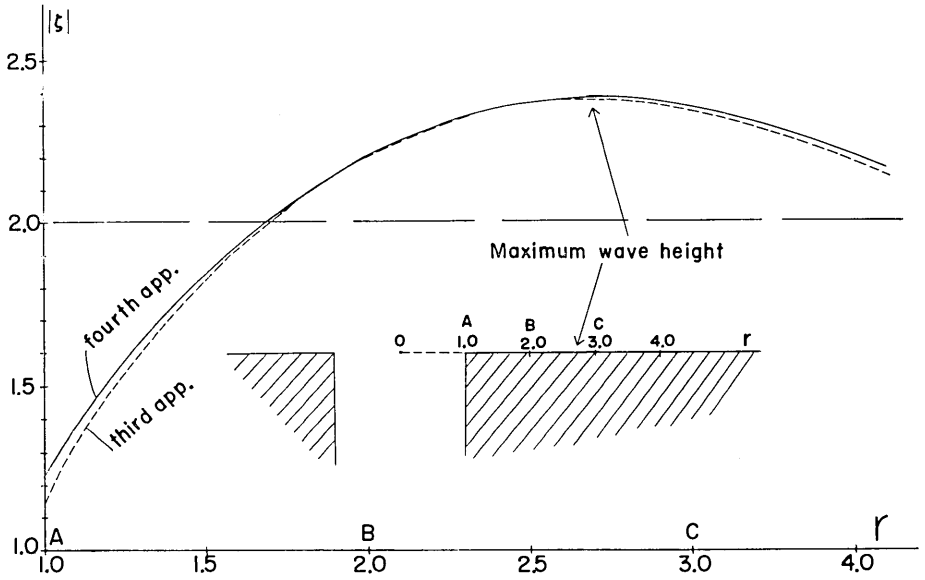

Fig. 19. A variation of the amplitude of waves for kd=1.4 along the straight coast.

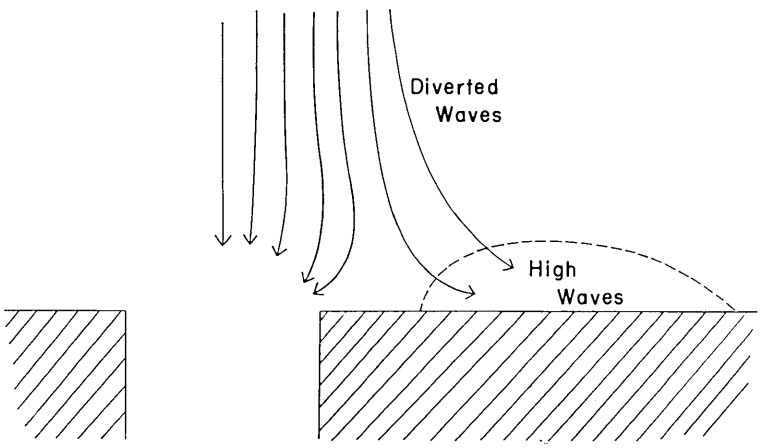

Fig. 20. A figurative explanation of high waves along the straight coast.

tude towards the straight coast facing the open sea, while, for the figures of $kd=1.0$ and 1.4 (Figs. 12 and 13), a trough appears in the offing which has a saddle as designated by "saddle part" in Fig. 18. Comparing Figs. 13 and 16, an appearance of a trough with a saddle part is considered to be a phenomenon beyond the error of the approximation. In Fig. 13, when one departs from an estuary along the straight coast, the magnitude of the amplitude is augmented gradually to exceed 2.0 which is an expected value when periodic waves invade perpendicularly to a straight coast. Such an excess is seen also in the figure (Fig. 16) based on the theory of the third approximation. For the behavior of the amplitude variation along the straight coast, Fig. 19 may be referred to, which is written for a parameter $kd=1.4$. According to the figure, a maximum of the amplitude appears at $r=2.7$ (a point nearby C in Fig. 19). The appearance of the maximum point is explained in such a way that the diverted waves (referring to Fig. 20) collide with the coast to produce high waves there.

---

51. 河口近傍における長波について [III]

地震研究所　桃　井　高　夫

前報告について河口近傍における長波に関する理論がベッセル函数の第 3，第 4，第 5 近似のもとに展開されている．理論展開の原理は筆者によって導入された buffer domain の方法である．そして次のような事実が新しく知られた．すなわち，

(1) 水路の内部に振巾の谷が見られる（これは前報告においては看過された事実である），

(2) 広海 (open sea) における振巾の谷線 (trough line) は河口に向って屈曲し，舌状の谷が河口の内部に入り込んでいる，

(3) 水路前面において等位相線は梯形をなしている，

(4) $kd=1.4$ (k: 波数，d: 水路の巾の半分の長さ）のとき，広海には河口よりそれてゆく波 (diverted wave) が現われ，直線海岸で高波をおこしながら海岸にそって進む．